Journal of Solid State Chemistry 184 (2011) 1666–1670

Contents lists available at ScienceDirect

Journal of Solid State Chemistry

journal homepage: www.elsevier.com/locate/jssc

# Synthesis and structure of $[C_6N_4H_{20}]_{0.5}[B_5O_6(OH)_4]$: A new organically templated pentaborate with white-light-emission

Yang Yang, Jiang-Bo Sun, Miao Cui, Rui-Bin Liu, Yu Wang, Chang-Gong Meng *

*Department of Chemistry, Dalian University of Technology, Dalian 116024, China*

ARTICLE INFO

*Article history:*
Received 24 February 2011
Received in revised form
27 April 2011
Accepted 1 May 2011
Available online 12 May 2011

*Keywords:*
Borate
Luminescence
White-light-emission

ABSTRACT

A new organically templated pentaborate $[C_6N_4H_{20}]_{0.5}[B_5O_6(OH)_4]$ (**1a**) was prepared by reactions of triethylenetetramine (TETA) with excess boric acid in aqueous solution and characterized by elemental analysis, FTIR, TG-DTA, powder X-ray diffraction and photoluminescence spectroscopy. The structure of **1a** was determined by a single-crystal X-ray diffraction. It crystallizes in the monoclinic system with space group $P2(1)/c$, $a=9200(3)$ Å, $b=14.121(5)$ Å, $c=10.330(4)$ Å, $\beta=91.512(4)^\circ$, $V=1341.4(9)$ Å$^3$, and $Z=4$. The luminescent properties of the compound were studied, and a green–blue luminescence occurs with an emission maximum at 507 nm upon excitation at 430 nm. The photoluminescence of **1a** can be modified from green–blue to white by means of a simple heat-treatment process. The white-light-emission of sample **1c** makes the pentaborate a good candidate for display and lighting applications in the white LED.



## 1. Introduction

Borate materials have attracted considerable attention in the past decades due to their rich structural chemistry and potential applications in mineralogy and industry [1–5]. Other important applications of borates are based on their optical properties, for example, nonlinear optics [6–9] and photoluminescence (PL) [10–12]. Since the discovery of the second-harmonic generation (SHG) properties of BBO (β-$BaB_2O_4$) [13] and LBO ($LiB_3O_5$) [14], many borate crystals, including $CsLiB_6O_{10}$ [15], $La_2CaB_{10}O_{19}$ [16], $BiB_3O_6$ [17], $Sr_2Be_2B_2O_7$ [9], $Pb_6B_{11}O_{18}(OH)_9$ [18], which show promising nonlinear optical properties, have been widely studied. The alkaline earth borates and rare-earth doped borates, such as $KCa_4(BO_3)_3$ [19], $LiBaBO_3:Sm^{3+}$ [20], $SrB_4O_7:Eu^{2+}$ [21], are an important luminescent material because of its excellent chemistry and thermal stabilization, facile synthesis and cheap raw material.

There is growing interest in developing white-light-emitting devices for applications in displays and lighting. One way to create white light source is to use multiple light-emitting diode (LED) chips, each emitting a different wavelength in close proximity to create the broad white light spectrum. The second method, phosphor-converted LEDs (pcLEDs) uses a single short wavelength LED (usually blue or ultraviolet) in combination with a phosphor, which absorbs a portion of the blue light and emits a broader spectrum of white light [22]. The most commercially popular white-light-emitting devices usually contain multiple emitting components, which have the following drawbacks: for example, rather complicated and expensive, white-emitting color changes with input power and poor stability. The way to solve these problems is using single-emitting-component (SEC) phosphors [23]. Thus far, most research work on SEC intrinsic white-light-emitting phosphors basically focuses on polymers, such as Si-based materials [24–28], polyfluorene derivatives [29–31], and inorganic materials doped with rare earth metal ions [32–36]. In contrast, the field of SEC white-light-emitting borate phosphors have seldom been investigated, only one example has been reported so far, namely $(H_2en)_2(Hen)_2B_{16}O_{27}$ (en=ethylenediamine) [23]. In this work, we report the synthesis and crystal structure of a new organically templated pentaborate, $[C_6N_4H_{20}]_{0.5}[B_5O_6(OH)_4]$ (**1a**). Notably, the photoluminescence of **1a** can be modified from green–blue to white by means of a simple heat-treatment process. The sample **1c** shows a white-light emission when illuminated with near-UV light. Therefore, this pentaborate could be a promising candidate for application in the white LED. The TETA molecule is often used as a ligand in the synthesis of metallo-organically templated borates, such as $[Co_2(TETA)_3][B_5O_6(OH)_4]_4$ [37], $[Zn(C_2H_3O_2)(TETA)][B_5O_6(OH)_4]$ [38], $[Cd(TETA)(C_2H_3O_2)][B_5O_6(OH)_4]$ [39]. In **1a**, the TETA molecules were diprotonated and located in the channels isolatedly as templates and counterions to compensate the negative charges of the framework.

## 2. Experimental section

### 2.1. Materials and physical measurements

All reagents were of analytical grade and were used as obtained by commercial sources without further purification. The elemental

* Corresponding author. Fax: +86 411 84708545.
*E-mail address:* cgmeng@dlut.edu.cn (C.-G. Meng).

0022-4596/$ - see front matter © 2011 Elsevier Inc. All rights reserved.
doi:10.1016/j.jssc.2011.05.001

analysis was carried out on an Elemental Vario EL III microanalyzer. Powder X-ray diffraction (XRD) data were recorded on a Shimazu X-ray diffractometer using Cu$K\alpha$ ($\lambda=1.5406$ Å) radiation (40 kV, 30 mA) with scanning rate of 0.06° $s^{-1}$, over the $2\theta$ range of 3–50°. IR spectra of the samples were recorded on Nicolet Avatar 360 FTIR spectrometer in the spectral region from 400 to 4000 $cm^{-1}$ with a resolution of 2 $cm^{-1}$ using the KBr technique. The thermal analysis was performed on a Mettler-Toledo SDTA 851 analyzer from ambient temperature to 1000 °C in $N_2$ atomsphere with a heating rate of 10 °C/min. The photoluminescence (PL) spectra were recorded at room temperature on Perkin Elmer LS-55 instrument, using 247 nm excitation line of the xenon laser as the excitation source. The photoluminescence images of **1a–c** were recorded using a fluorescent microscope (Olympus BX51).

### 2.2. Synthesis and heat treatment

The title compound was prepared by adding boric acid (18.54 g, 0.3 mol) to a solution of triethylenetetramine (3.75 g, 0.03 mol) in 150 mL of deionized water. This mixture was heated to 90 °C with stirring in a water bath, then evaporated and condensed to about 50 mL, after that a transparent pale yellow liquid was obtained. The liquid was filtered and heated to evaporate gradually in a 45 °C of water bath to allow crystalline products to slowly form. Large single crystals were obtained after 1 week. The resulting yellowish block crystals of **1a** (65.4% yield based on boron) were collected by filtration, successively washed with distilled water and absolute ethyl alcohol, and dried at 60 °C in air. Elemental analysis (%) calcd. for **1a**: C 12.33, H 4.83, N 9.59; Found: C 12.45, H 4.79, N 9.62. The X-ray powder diffraction pattern for the bulk product is in good agreement with the pattern based on single-crystal X-ray solution in position, indicating the phase purity of the as-synthesized samples of the title compound (Supporting information, Fig. S1).

Heat treatment of **1a**: A yellowish solid sample of **1a** was placed in an $Al_2O_3$ crucible, which was heated to 200 °C in a programmable furnace at a rate of 5 K $min^{-1}$, followed by a 3-h isothermal hold, after which it was cooled to room temperature to yield pale yellow **1b**. Khaki **1c** and puce **1d** were obtained as for **1b** except that the temperature was changed to 250 and 300 °C, respectively.

### 2.3. Crystallographic studies

A suitable single crystal of **1** with the dimensions of 0.10 × 0.25 × 0.25 $mm^3$ was carefully selected under an optical microscope and glued to thin glass fiber with epoxy resin. The intensities of the crystal data were collected on a Bruker SMART APEX CCD diffractometer with graphite–monochromated Mo$K\alpha$ ($\lambda=0.71073$ Å) using the SMART and SAINT programs [40]. All structure solutions were performed with direct methods using SHELXS-97 [41] and the structure refinement was done against $F^2$ using SHELXL-97 [42]. All non-hydrogen atoms were found in the final difference Fourier map and refined with anisotropic thermal displacement coefficients except C3. All hydrogen atoms were fixed geometrically at calculated distances and allowed to ride on the parent non-hydrogen atoms. Crystallographic data (excluding structure factors) for the structure reported in this paper have been deposited with the Cambridge Crystallographic Data Centre as supplementary publication no. CCDC No. 806358. Copies of the data can be obtained free of charge on application to CCDC, 12 Union Road, Cambridge CB2 1EZ, UK (fax: +44 1223 336 033; e-mail: mailto:mdeposit@ccdc.cam.ac.uk). Some refinement details and crystal data of **1a** are summarized in Table 1. Selected bond lengths and bond angles are listed in Table S1 in the Supplementary materials.

**Table 1**
Crystallographic data of **1a**.

| | |
|---|---|
| Formula | $C_3H_{14}B_5N_2O_{10}$ |
| Formula weight | 292.21 |
| Temperature (K) | 293(2) |
| Wavelength (Å) | 0.71073 |
| Crystal system | Monoclinic |
| Space group | $P2(1)/c$ |
| $a$ (Å) | 9.200(3) |
| $b$ (Å) | 14.121(5) |
| $c$ (Å) | 10.330(4) |
| $\beta$ (deg.) | 91.512(4) |
| Volume (Å$^3$) | 1341.4(9) |
| $Z$ | 4 |
| $\rho_{calcd}$ (g $cm^{-3}$) | 1.447 |
| $\mu$(Mo$K\alpha$) ($mm^{-1}$) | 0.13 |
| $F$(0 0 0) | 604 |
| Limiting indices | $-10\le h\le 10,\ -9\le k\le 16,\ -12\le l\le 12$ |
| Weighting scheme | $w=1/[\sigma^2(F_o^2)+(0.1983P)^2]$ where $P=(F_o^2+2F_c^2)/3$ |
| Reflections collected | 6027 |
| Independent reflections | 2320 |
| Independent reflections with $I>2\sigma(I)$ | 1704 |
| $R_{int}$ | 0.026 |
| Completeness to $\Theta=24.99$ | 98.2% |
| Refinement method | Full-matrix least-squares on $F^2$ |
| Goodness-of-fit on $F^2$ | 1.00 |
| Final $R$ indices [$I>2\sigma(I)$] | $R_1=0.0735$, w$R_2=0.225$ |

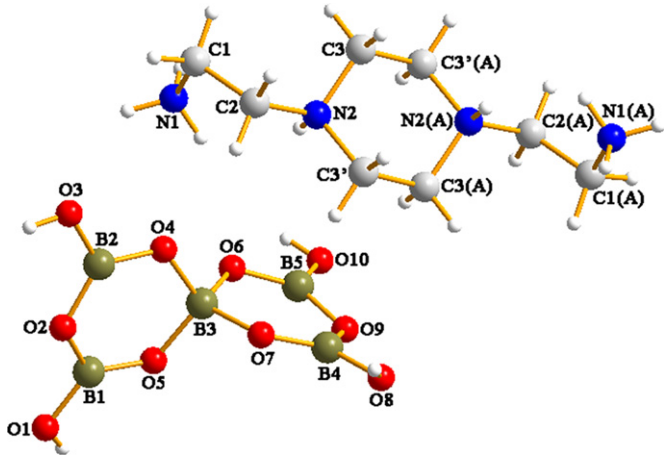


**Fig. 1.** Ball–stick view and atomic labeling scheme for an asymmetric unit of **1a**. Atom labels with "A" refer to symmetry-generated atoms.

## 3. Results and discussion

### 3.1. Crystal structure

The asymmetric unit of **1a** contains one $[B_5O_6(OH)_4]^-$ anion and one half $[C_6N_4H_{20}]^{2+}$ cation (Fig. 1). The cation is symmetric and contains one disordered carbon atom, C3 with an equal site-occupation factor (SOF) of 0.5. The structure of the polyborate anion $[B_5O_6(OH)_4]^-$ is composed of four $BO_3$ triangles and one $BO_4$ tetrahedron linked to each other. This isolated pentaborate anion is characterized by two rings $[B_3O_3]$ linked by a common $BO_4$ tetrahedron. Each ring is produced by two $BO_3$ triangles and a slightly distorted common $BO_4$ tetrahedron. The terminal oxygen atoms are protonated. The B–O distances for the trigonal boron atoms are between 1.339(4) and 1.395(4) Å [av.=1.363 Å], and the B–O distances for the tetrahedral boron atom range from 1.459(4) to 1.486(4) [av.=1.471 Å]. The O–B–O angles involving trigonal boron

atoms are in the range of 116.2(3)–123.2(3)° and the O–B–O angles involving tetrahedral are in the range of 108.0(3)–111.3(2)°.

It is known that multipoint hydrogen bond interactions play an important role in the formation and stability of low-dimensional structures [43–45]. As expected to be a common fundamental building block (FBB) for supramolecular hydrogen bonded structure, the polyanion $[B_5O_6(OH)_4]^-$ is connected with each other to form three-dimensional (3D) hydrogen-bonded architecture by –OH groups oriented in a planar triangular fashion in many pentaborates [46–48]. The common 3D hydrogen-bonded architecture is a unidirectional rectangle-like borate anion host lattice with 12-membered boron rings channels as shown in Fig. S2. Although the title compound also contains $[B_5O_6(OH)]^-$ polyborate anions, the hydrogen bonding borate anion host lattice is distinct from the structures of other pentaborate. One of the noticeable characteristics is that the 12-membered boron ring which was built of six $[B_5O_6(OH)]^-$ polyborate anions through hydrogen bonds is parallelogram-like approximately, as shown in Fig. 2a, and these rings link each other to form the parallelogram-like channels which are paratactic distributed along the *x*-axis (Fig. 2b). The diprotonated organic molecules $H_2$TETA, are located at the channels to compensate the negative charges and interacted with the inorganic framework through extensive hydrogen-bonds with N…O distance in the range of 2.876–3.307 Å (Fig. 2c, d). Another interesting characteristic is that the $[B_5O_6(OH)_4]^-$ unit is connected to four neighboring units by O–H…O hydrogen bonds, forming 8-membered boron rings, as shown in Figs. 3a and 4b, and these puckered rings are linked together by hydrogen bonds to form the channels along the *z*-axis (Fig. 3c). Details of H-bonds are given in Table S2.

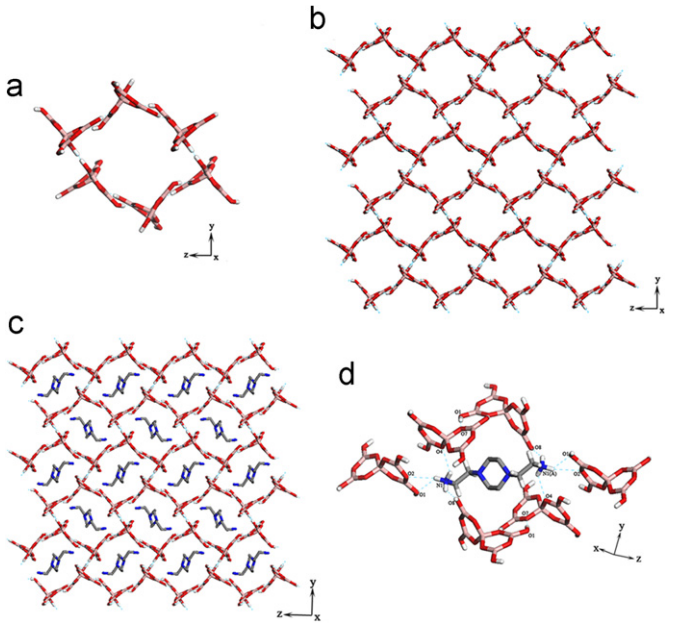


**Fig. 2.** (a) View of the 6-membered boron rings constructed by H-bonding. (b) View of the hydrogen bonded architectures of **1a** along the *x*-axis. (c) View of the packing structure of **1a** along the *x*-axis. Hydrogen atoms of the cations are omitted for clarity. (d) Side view of the H-bonds interaction between the $[C_6N_4H_{20}]^{2+}$ cation and adjacent $[B_5O_6(OH)_4]^-$ clusters in **1a**. Hydrogen atoms of the disordered carbon atoms are omitted for clarity.

### 3.2. Infrared (IR) spectra

The IR spectrum of **1a** is shown in Fig. S3. The stretching vibrations of the O–H, C–H, and N–H bands are observed at 3342, 3176, 2967, 2829 $cm^{-1}$. The two weak bands at 1628 $cm^{-1}$ are related to the bending of $-NH_2$. The strong bands at 1410, 1321 and 929 $cm^{-1}$ are the asymmetric and symmetric stretching modes of B–O in $BO_3$, while the bands at 1135, 1062, 1021, and 779 $cm^{-1}$ are characteristic of the asymmetric and symmetric stretching modes of B–O in $BO_4$ [49–51], and the stretching vibrations of the C-N band are also located around 1062 $cm^{-1}$. The band at 1200 $cm^{-1}$ is related to the in-plane bending mode of B–O–H group. The out-of-plane bending mode of B–O in $BO_3$ is present at 700 $cm^{-1}$.

### 3.3. Thermal properties

The thermal behavior of **1a** was shown in Fig. S4. The TG curve of **1a** illustrated that the compound was stable up to about 235 °C. On further heating a continuous weight loss of 37.83% between 235 and 600 °C was observed, corresponding to the removal of the organic amine (calcd. 25.37%) and two water molecules from the dehydration of hydroxyls (calcd. 12.32%). This result is identical with the structural refinement of single crystal X-ray diffraction. In the DTA curve, there are three endothermic peaks. The first two adjacent endothermic peaks at 282 and 299 °C are attributed to the removal of the organic amine, while the third endothermic peak at 486 °C is related to the dehydration of hydroxyl. The solid samples **1b–d** were heat-treated at 200, 250 and 300 °C, respectively.

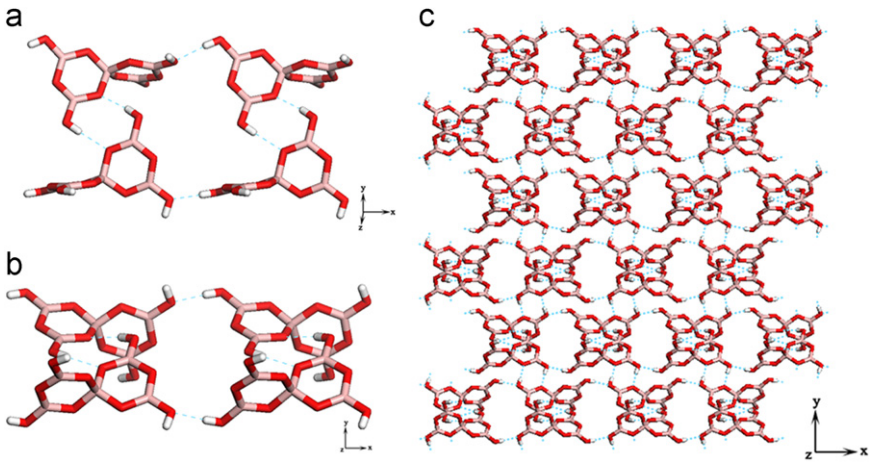


**Fig. 3.** (a) Side view of the 8-membered boron ring; (b) view of the 8-membered boron ring along the *z*-axis and (c) view of the hydrogen-bonded borate anion host lattice with 8-membered boron rings along the *z*-axis.

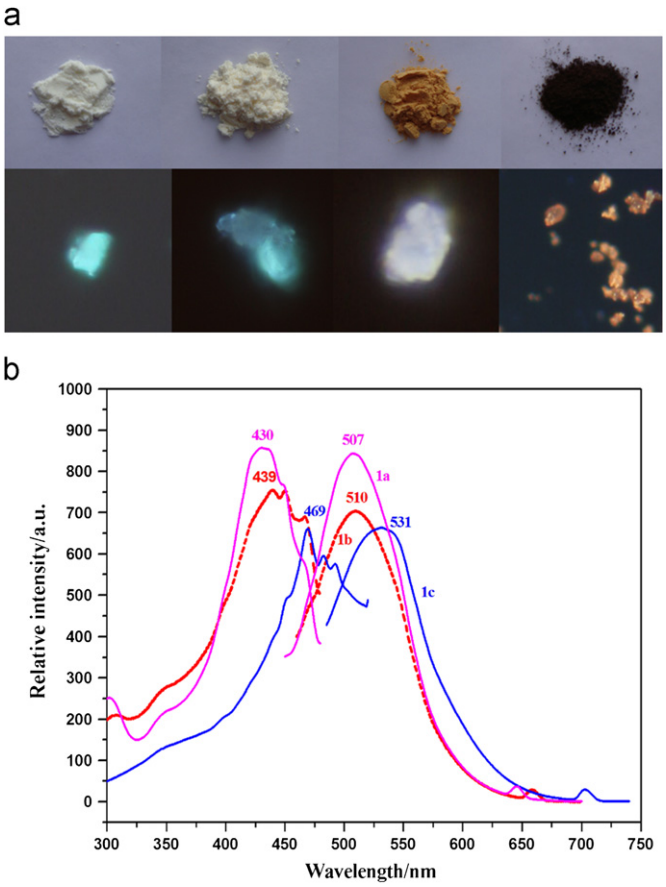


**Fig. 4.** (a) Images of the solid samples of **1a**–**d** (top left to right) and their corresponding photoluminescence when illuminated with near-UV light at room temperature and (b) solid-state PL spectra of **1a**–**c** at room temperature.

The powder X-ray diffraction patterns show that the framework is retained up to 200 °C, which agrees with the TG analysis, and above 250 °C, it collapses and decomposes to amorphous $B_2O_3$ (Fig. S5).

### 3.4. Variable temperature luminescent properties

Heat treatment of yellowish **1a** yields pale yellow **1b** at 200 °C, khaki **1c** at 250 °C and puce **1d** at 300 °C (Fig. 4a). Interestingly, solid samples **1a**–**c** display green–blue, green–blue, and white photoluminescence, respectively, when illuminated with near-UV light (Fig. 4a). Fig. 4b shows the emission and excitation spectra of solid samples **1a**–**c**. As can be seen from the figure, compound **1a** can be excited by light with a wavelength ranging from 325 to 475 nm, a green–blue photoluminescence phenomenon occurs with an emission maximum at 507 nm upon excitation at 430 nm. It is noted that the emission spectrum of **1b** has a 3 nm red shift compared with that of **1a**, while an obvious red shift with 24 nm of **1c** is found when compared with that of **1a**. At the same time, with the rise of the heat-treatment temperature the excitation spectra of solid samples **1b** and **1c** also have red shift with 9 and 39 nm, respectively compared with that of **1a**. It is worth noting that the emission and excitation spectra of solid samples **1a**, **b** only have small changes, which is consistent with that **1b** has an almost the same PXRD pattern to **1a** (Fig. S5). When heat-treatment temperature rises to 250 °C, the framework in **1c** has partial collapsed (Fig. S5), which is in accordance with the obvious red shift of the emission and excitation spectrum compared with that of **1a**. When the temperature is up to 300 °C, the ammonium ions removed and the framework has collapsed in **1d**, so we did not observe the luminescence when illuminated with near-UV light. Thus, the PL of **1a**–**c** should originate from the borate framework rather than the isolated ammonium ions. Since no metal activator ions exist in the sample, the self-activating PL of **1b**, **c** probably originate from structural defects caused by heat treatment.

## 4. Conclusions

In summary, we have prepared a new organically templated pentaborate $[C_6N_4H_{20}]_{0.5}[B_5O_6(OH)_4]$ (**1a**) with TETA molecules as template in aqueous solution. A novel framework was obtained from $[B_5O_6(OH)_4]^-$ units through hydrogen bonds interaction. The photoluminescence of **1a** can be modified from green–blue to white by means of a simple heat-treatment process. Compound **1c** is a new intrinsic white SEC phosphor in the borate system. Facile synthesis, moderate thermal stability, easy separation, zero metal content and white-light-emission of sample **1c** make the penatborate a good candidate for display and lighting applications in the white LED.

## Appendix. Supplementary data

Crystallographic data (CIF), selected bond lengths and angles, details of hydrogen bonds, FTIR spectra, simulated and experimental PXRD patterns, and TG-DTA curves are provided as supplementary materials.

## Acknowledgments

We are grateful to Dr. Cheng He and Dr. Yuan Lin for assistance with the single-crystal X-ray diffraction and photoluminescence studies, respectively.

## Appendix A. Supplementary material

Supplementary data associated with this article can be found in the online version at doi:10.1016/j.jssc.2011.05.001.

## References

[1] C.L. Christ, J.R. Clark, Phys. Chem. Miner. 2 (1997) 59.
[2] P.C. Burns, J.D. Grice, F.C. Hawthorne, Can. Miner. 33 (1995) 1131.
[3] P.C. Burns, Can. Miner. 33 (1995) 1167.
[4] J.D. Grice, P.C. Burns, F.C. Hawthorne, Can. Miner. 37 (1999) 731.
[5] G. Heller, Top. Curr. Chem. 131 (1986) 39.
[6] P. Becker, Adv. Mater. 10 (1998) 979.
[7] T. Sasaki, Y. Mori, M. Yoshimura, Y.K. Yap, T. Kamimura, Mater. Sci. Eng. 30 (2000) 1.
[8] F. Kong, S.P. Huang, Z.M. Sun, J.G. Mao, W.D. Cheng, J. Am. Chem. Soc. 128 (2006) 7750.
[9] C.T. Chen, Y.B. Wang, B.C. Wu, K.C. Wu, W.L. Zeng, L.H. Yu, Nature 373 (1995) 322.
[10] T. Jüstel, H. Nikol, C. Ronda, Angew. Chem. Int. Ed. 37 (1998) 3084.
[11] W.G. Shu, L.Z. Zheng, Z.C. Zhou, Chin. Rare Earths 23 (2002) 77.
[12] H.Y. Lin, W.P. Qin, J.S. Zhang, Ch.F. Wu, Solid State Commun. 141 (2007) 436.
[13] C. Chen, B. Wu, A. Jiang, G. You, Sci. Sin. B 28 (1985) 235.
[14] C. Chen, Y. Wu, A. Jiang, B. Wu, G. You, R. Li, S. Lin, J. Opt. Soc. Am. B 6 (1989) 616.
[15] Y. Mori, I. Kuroda, S. Nakajima, T. Sasaki, S. Nakai, Appl. Phys. Lett. 67 (1995) 1818.
[16] Y.C. Wu, J.G. Liu, P.Z. Fu, J.X. Wang, H.Y. Zhou, G.F. Wang, C.T. Chen, Chem. Mater. 13 (2001) 753.
[17] H. Hellwig, J. Liebertz, L. Bohaty, J. Appl. Phys. 88 (2000) 240.
[18] Z.T. Yu, Z. Shi, Y.S. Jiang, H.M. Yuan, J.S. Chen, Chem. Mater. 14 (2002) 1314.
[19] L. Wu, X.L. Chen, Y.P. Xu, Y.P. Sun, Inorg. Chem. 45 (2006) 3042.
[20] P.L. Li, Z.J. Wang, Z.P. Yang, Q.L. Guo, X. Li, Mater. Lett. 63 (2009) 751.
[21] K. Machid, G. Adachi, J. Shiokawa, J. Lumin. 21 (1979) 101.

[22] Farheen N. Sayed, V. Grover, K.A. Dubey, V. Sudarsan, A.K. Tyagi, J. Colloid Interface Sci. 353 (2011) 445.
[23] M.S. Wang, G.C. Guo, W.T. Chen, G. Xu, W.W. Zhou, K.J. Wu, J.S. Huang, Angew. Chem., Int. Ed. 46 (2007) 3909.
[24] W.H. Green, K.P. Le, J. Grey, T.T. Au, M.J. Sailor, Science 276 (1997) 1826.
[25] T. Uchino, T. Yamada, Appl. Phys. Lett. 85 (2004) 1164.
[26] T. Hayakawa, A. Hiramitsu, M. Nogami, Appl. Phys. Lett. 82 (2003) 2975.
[27] K.L. Paik, N.S. Baek, H.K. Kim, J.H. Lee, Y. Lee, Macromolecules 35 (2002) 6782.
[28] L.D. Carlos, R.A. Sá Ferreira, R.N. Pereira, M. Assuncüão, V. de Zea Bermudez, J. Phys. Chem. B 108 (2004) 14924.
[29] S.K. Lee, D.H. Hwang, B.J. Jung, N.S. Cho, J. Lee, J.D. Lee, H.K. Shim, Adv. Funct. Mater. 15 (2005) 1647.
[30] G. Tu, Q. Zhou, Y. Cheng, L. Wang, D. Ma, X. Jing, F. Wang, Appl. Phys. Lett. 85 (2004) 2172.
[31] G. Tu, C. Mei, Q. Zhou, Y. Cheng, Y. Geng, L. Wang, D. Ma, X. Jing, F. Wang, Adv. Funct. Mater. 16 (2006) 101.
[32] B. Liu, C. Shi, Z. Qi, Appl. Phys. Lett. 86 (2005) 191111.
[33] Y.Q. Li, G. deWith, H.T. Hintzen, J. Mater. Chem. 15 (2005) 4492.
[34] S. Sivakumar, F.C.J.M. van Veggel, M. Raudsepp, J. Am. Chem. Soc. 127 (2005) 12464.
[35] Y. Mita, T. Kobayashi, Y. Miyamoto, O. Ishii, N. Sawanobori, Phys. Stat. Sol. B 241 (2004) 2672.
[36] W. Yang, T.M. Chen, Appl. Phys. Lett. 88 (2006) 101903.
[37] G.M. Wang, Y.Q. Sun, G.Y. Yang, J. Solid State Chem. 179 (2006) 1545.
[38] S.L. WU, H.X. Liu, X. Jiang, Z.D. Shao, Y.X. Liang, Acta Cryst. C 65 (2009) 308.
[39] Y. Yang, Y. Wang, J.B. Sun, M. Cui, C.G. Meng, Z. Anorg. Allg. Chem. 201000410, in press.
[40] SMART and SAINT, Area Detector Control and Integration Software, Siemens Analytical X-Ray Systems, Inc., Madison, WI, 1996.
[41] G.M. Sheldrick, SHELXS-97: Program for Crystal Structure Solution, University of Göttingen, Germany, 1997.
[42] G.M. Sheldrick, SHELXL-97: Program for the Refinement of Crystal Structures, University of Göttingen, Germany, 1997.
[43] D.M. Schubert, M.Z. Visi, C.B. Knobler, Inorg. Chem. 47 (2008) 2017.
[44] H.X. Liu, Y.X. Liang, X. Jiang, J. Solid State Chem. 181 (2008) 3243.
[45] D.M. Schubert, M.Z. Visi, C.B. Knobler, Inorg. Chem. 47 (2008) 4740.
[46] G.M. Wang, J.H. Li, Z.X. Li, P. Wang, H. Li, Z. Anorg. Allg. Chem. 634 (2008) 1192.
[47] G.M. Wang, Y.Q. Sun, G.Y. Yang, J. Solid State Chem. 178 (2005) 729.
[48] Z.H. Liu, J.J. Zhang, W.J. Zhang, Inorg. Chim. Acta 359 (2006) 519.
[49] C.E. Weir, J. Res. Nafl. Bur. Stand. Sect. A 70A (1996) 153.
[50] C.E. Weir, R. Schroeder, J. Res. Nafl. Bur. Stand. Sect. A 68A (1964) 465.
[51] J. Krogh-Moe, Phys. Chem. Glases 6 (1965) 46.